Quantum Electronics **50** (9) 850–854 (2020)

LASER SPECTROSCOPY https://doi.org/10.1070/QEL17373

Compact ultrastable laser system for spectroscopy of $^2S_{1/2} \rightarrow {}^2D_{3/2}$ quadrupole transition in $^{171}Yb^+$ ion

I.V. Zalivako, I.A. Semerikov, A.S. Borisenko, M.D. Aksenov, P.A. Vishnyakov, P.L. Sidorov, N.V. Semenin, A.A. Golovizin, K.Yu. Khabarova, N.N. Kolachevsky

Abstract. **We report the results of studying a compact laser system designed for manipulating a quantum state of the optical qubit based on the $^2S_{1/2} \rightarrow {}^2D_{3/2}$ quadrupole transition in the $^{171}Yb^+$ ion at a wavelength of 435.5 nm. An emission power of the laser system reaches 500 μW at $\lambda = 435.5$ nm and the relative frequency instability of at most 3×10^{-15} is achieved at averaging intervals from 0.5 to 50 s with a subtracted linear frequency drift. The compactness of the developed system makes it possible to employ it in transportable systems including optical clocks.**

Keywords: *laser spectroscopy, optical qubit, quadrupole transition, $^{171}Yb^+$ ion.*

1. Introduction

In last two decades, much attention has been paid to quantum computations and quantum simulations by scientific community and industrial companies, which is explained by the impressive success in this field. Quantum simulators have been created which include several tens qubits based on neutral atoms and ions [1, 2]. A prototype of a universal quantum computer comprised of 17 qubits on $^{171}Yb^+$ ions has also been developed [3, 4]. Google reported attaining the so-called "quantum supremacy" on its Sycamore comprised of 53 superconducting qubits [5], and Honeywell announced in 2019 an ion quantum computer with a record quantum volume [6] exceeding 64 [7]. In the same year, PsyQuantum startup also reported that they are ready to demonstrate a system with a million physical qubits on silicon photonic chips within the next few years. Many developed quantum computer prototypes are now in open access through cloud technologies. Many companies including Google, Volkswagen, Airbus, and Microsoft declare the employment of quantum computers in the near future or even presently [5, 8].

I.V. Zalivako, I.A. Semerikov, A.S. Borisenko, M.D. Aksenov, P.A. Vishnyakov, P.L. Sidorov, A.A. Golovizin Lebedev Physical Institute, Russian Academy of Sciences, Leninsky prosp. 53, 119991 Moscow, Russia; e-mail: zalivako.ilya@yandex.ru;
N.V. Semenin Moscow Institute of Physics and Technology, Institutskii per. 9, 141701 Dolgoprudnyi, Moscow region, Russia;
K.Yu. Khabarova, N.N. Kolachevsky Lebedev Physical Institute, Russian Academy of Sciences, Leninsky prosp. 53, 119991 Moscow, Russia; Russian Quantum Centre, Bol'shoi bul. 30, stroenie 1, Skolkovo, 121205 Moscow, Russia

Received 26 May 2020
Kvantovaya Elektronika **50** (9) 850–854 (2020)
Translated by N.A. Raspopov

Presently, there are several promising hardware platforms for quantum computations competing with each other. These are superconducting circuits [5, 6], ions in traps [9], neutral atoms [10], and photons [11]. Each of the platforms has advantages and drawbacks and it is not clear which one will be the leader. For example, ion quantum computers have the longest coherence time [12], straightforward way for performing quantum operations [13], and highly reliable preparation and readout of a quantum state [14]; however, such systems are technically difficult to scale. Nevertheless, methods are suggested for overcoming these difficulties [4, 15, 16]. Later on, we will dwell on this particular platform for quantum computations.

In ion, qubits can be encoded in an optical transition, hyperfine sublevels of the ground state, or in Zeeman components. The first two approaches are most popular. Microwave qubits on hyperfine components exhibit a long coherence time; however, optical qubits are simpler in individual addressing and provide more reliable data preparation and readout. Up to now, microwave qubits have been realised on a series of ions, for example, Yb^+ [17], Be^+ [13], Mg^+ [18], Ca^+ [14], Sr^+ [19], whereas an optical qubit has only been realised on Ca^+ [14] and Sr^+ [20] ions.

Ion $^{171}Yb^+$ is now widely used in quantum computations and metrology. This is explained by the structure of electron levels, which allows one to employ direct laser cooling of this element by diode laser sources without nonlinear frequency conversion. A microwave qubit can be realised on the transition between hyperfine components of the ground state at the frequency of 12.6 GHz. In addition, this ion has the optical $^2S_{1/2}(F = 0) \rightarrow {}^2D_{3/2}(F = 2)$ quadrupole transition at a wavelength $\lambda = 435.5$ nm and $^2S_{1/2}(F = 0) \rightarrow {}^2F_{7/2}(F = 3)$ octupole transition at $\lambda = 467$ nm with the natural spectral widths of 3.1 Hz and ~1 nHz, respectively. These transitions are widely used in metrology and are promising candidates for optical qubits.

A long lifetime of the excited state and weak sensitivity to external fields stipulate for its employment in clock standards and improve optical qubit characteristics as well.

In the present work, we present the results of investigating a laser system designed for manipulating a quantum state of the optical qubit based on the $^2S_{1/2}(F = 0) \rightarrow {}^2D_{3/2}(F = 2)$ quadrupole transition in ion $^{171}Yb^+$ aimed at studying the possibility of developing a scalable ion quantum computer on this basis. Such a laser system should emit the radiation at $\lambda = 435.5$ nm with a high frequency stability for realising efficient excitation of the transition and supressing qubit dephasing. The frequency stabilisation system is a significantly improved version of ultrastable laser systems developed earlier in our laboratory [21] and used in spectroscopy

of clock transitions in thulium [22] and strontium [21] atoms. While developing the frequency stabilisation system, the main attention was paid to make it compact with good mass-dimension characteristics without worsening the metrological properties. In a result, an autonomous easily transportable system was developed, which is important for practical applications. A number of laboratories in the world work on similar problems including mounting ultrastable systems aboard a spacecraft for reducing phase noise and increasing the accuracy of cosmic ranging [23]. The relevance of such systems in commercial applications is illustrated by a prototype of an ion quantum computer (IonQ company) realised as an autonomous device with a volume of several cubic metres. Such systems are also needed for developing transportable optical frequency standards; this field is actively developed in the Russian Federation [24, 25] and other countries [26–28]. In the present paper, we describe our laser system and present results of its comparison with our earlier laser system designed for spectroscopy of the clock transition in thulium atoms at a wavelength of 1140 nm by means of a femtosecond optical frequency comb.

2. Laser system

The laser system schematically shown in Fig. 1 is arranged on a single optical breadboard of size 40 × 40 cm. For improving the mass-dimension characteristics, it was assembled using half-inch optics; the employed aluminium breadboard had a honeycomb structure. The system developed was based on a semiconductor laser with an external cavity Toptica DLC Pro. The laser with an output power of 80 mW at a wavelength of 871 nm included a 60-dB embedded optical isolator for suppressing the influence of reflected radiation to the frequency of output radiation. The laser emission, after its spatial profile was corrected by an anamorphic prism pair, is split into three parts. The first part passes through an optical fibre to a frequency doubler for providing an output signal at a wavelength of 435.5 nm. The second part also passes to an optical fibre and is used for studying frequency stability of the laser system. The third part is used for stabilising the laser emission frequency with respect to a high-finesse optical cavity.

The optical frequency is doubled by using an AdvR WSH-K0436-P85P40AL3 fibre device. The employment of the waveguide in a periodically polarised nonlinear crystal provides a high conversion efficiency without cavity and significantly simplifies the construction. The device converts an input radiation with the power of 35 mW at a wavelength of 871 nm into a double-frequency radiation with the power of 500 μW.

An emission wavelength of the laser system was monitored by a WS8-2 precision wavemetre calibrated to the clock transition frequency of thulium atoms [22], which provides the accuracy of laser source frequency measurements better than 10 MHz. In addition, for studying the frequency stability, part of the laser radiation is diverged for comparison with a femtosecond frequency comb. It will be described in more details below.

The remaining radiation is used for stabilising the laser system frequency relative to a high-finesse cavity. Locking of the laser frequency to the cavity mode was realised using the Pound–Drever–Hall technique [29]. At first, the beam passes through an acousto-optical modulator (AOM) in the double-pass configuration. Firstly, this provides detuning of the laser system frequency from the optical cavity mode and, secondly, prevents arising parasitic interferometers between the cavity input mirror and optical components prior to the AOM. In addition, the power of radiation passed to the cavity is actively stabilised by the same AOM. The laser beam that passes to the cavity is spatially matched with the TEM_{00} mode. Reflected and transmitted signals are detected by photodi-

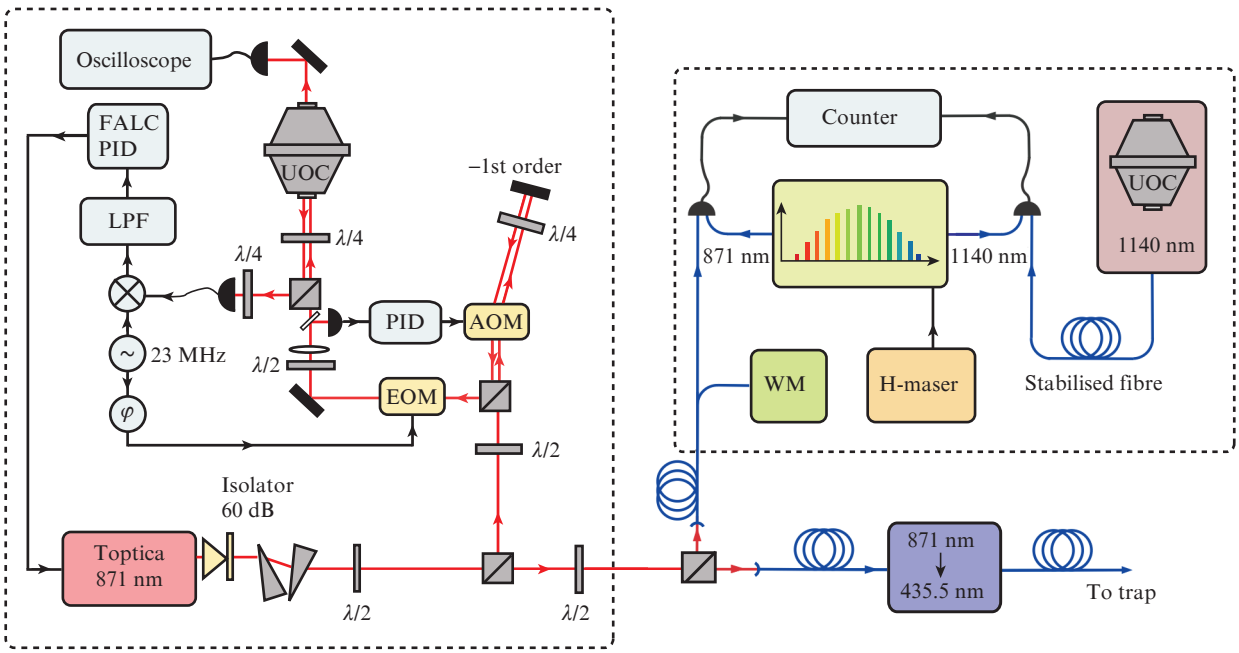

Figure 1. Schematic of the laser system and experiment on studying frequency stability relative to the reference laser system at a wavelength of 1140 nm:
(WM) precision wavemetre; (H-maser) passive hydrogen maser; (PID) proportional-integral-differential amplifier; (UOC) ultrastable optical cavity (ULE glass); (EOM, AOM) electro- and acousto-optical modulators; (LPF) low-pass filter.

odes. A quarter-wave plate is placed in front of the photodiode that detects the reflection signal for suppressing an influence of a parasitic interferometer formed by reflection from a detector surface.

According to the Pound–Drever–Hall method, the laser beam prior to the cavity is phase-modulated by an electro-optical modulator (EOM). A signal from the photodiode detecting the reflected beam is amplified and mixed with a reference signal of the same frequency, thus, forming the error signal. The latter signal passes to a fast FALC 110 PID-controller, which controls the diode laser current and closes the feedback loop. An additional 'slow' output from the PID-controller also provides a feedback signal to the laser piezoactuator and compensates for slow substantial frequency deviations. In this configuration, the feedback bandwidth is 1.2 MHz and is determined by the locking electronics.

3. High-finesse optical cavity

As compared to the previous-generation ultrastable laser systems described in [21, 30], the principal updates affected the cavity vacuum chamber. In the present work, an optical cavity is used which body is fabricated from ULE (Ultra Low Expansion) glass and geometry is similar to that described in [30]. The glass is specific in that there is a 'zero point' near room temperature at which the linear expansion coefficient turns to zero and the dependence of a cavity length on temperature substantially weakens. Highly reflecting mirrors (SIGMAKOKI) operating at a wavelength of 871 nm are mounted on the cavity body by using the optical contact technique. The used cavity differs from that described in [30] in that the mirror substrates are made of fused silica instead of ULE glass. Fused silica has a higher mechanical Q-factor, which reduces the contribution of thermal noise into laser instability [31]. However, due to the difference in silica and ULE thermal expansion coefficients, a temperature variation induces an additional mechanical stress in the domain of the optical contact between two materials and the cavity length changes. In the result, the position of the effective 'zero point' where the first temperature derivative of the cavity length turns to zero, shifts by 10–20 °C to lower temperatures [32]. In view of this fact, the vacuum chamber was designed with the possibility of temperature stabilisation in the range from 0 to 20 °C.

The quality of cavity mirror fabrication was tested by measuring the cavity finesse according to the "ring-down" technique [33]. The finesse was 120000 which corresponds to the cavity linewidth (FWHM) of ~16 kHz. Unfortunately, the cavity transmission was rather low (about 0.3%) even at the optimal mode-matching; this confirms high losses on the mirrors.

The vacuum chamber is schematically shown in Fig. 2. It still has three thermal shields for cavity thermal isolation and suppressing temperature gradients arising in the chamber material. The cavity mount is also similar to those described earlier. Geometrical dimensions and gaps between the screens are reduced and the method of shield mounting is changed. Temperature is stabilised by using a Peltier element placed between the shields and a temperature sensor. In addition, the ion-getter pump with the pumping rate of 10 L s^{-1} used in our previous systems has been replaced with two ion pumps possessing the pumping rate of 3 L s^{-1} each (one pump is Gamma Vacuum TiTan 3S and the other with similar characteristics is produced by Vremya-Ch). This noticeably reduced the size and mass of the system.

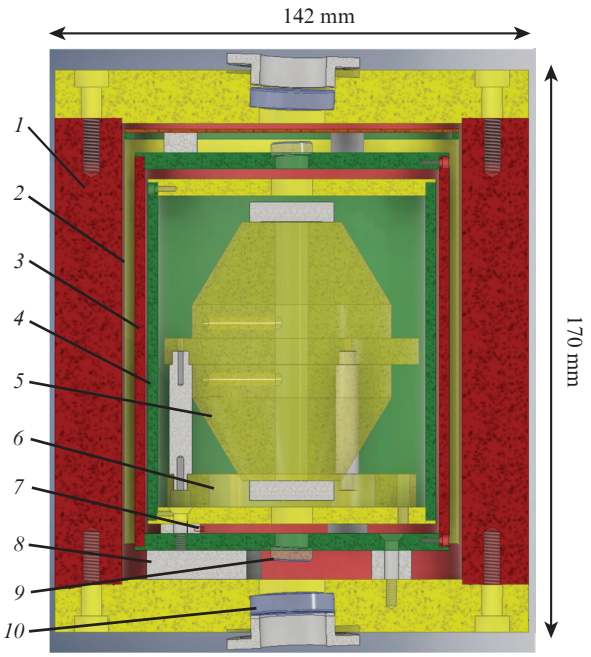

Figure 2. Compact vacuum chamber with an optical cavity: (*1*) external aluminium chamber; (*2*) first ('thin') thermal shield; (*3*) second thermal shield; (*4*) third thermal shield; (*5*) high-finesse optical cavity; (*6*) Zerodur ring; (*7*) temperature sensor mounted in an aluminium post; (*8*) Peltier element; (*9*, *10*) antireflection optical windows.

Measurements performed have shown that the changes in construction do not worsen characteristics of the vacuum chamber. The new pump configuration provided a pressure of about 4×10^{-8} mbar (according to a pump controller) and the time response of cavity temperature change under a stepwise variation of the reference temperature was at least 4 hours. The mass and volume of the assembled vacuum chamber were reduced to 7 kg and 3.5 L, respectively (in the previous system these were 20 kg and 10 L).

4. Study of the frequency stability of laser system radiation

Stability characteristics of the laser system at $\lambda = 871$ nm were studied through variations of its frequency relative to the hydrogen radio-frequency source – a passive hydrogen maser and a clock laser used for spectroscopy of thulium atoms [22] at $\lambda = 1.14$ μm. For comparison, a fibre femtosecond frequency comb (Avesta) was used equipped with optical outputs at both mentioned wavelengths. The radiation of both laser systems was mixed with the optical comb radiation by means of balance heterodyning [34]. A zero-dead-time counter K + K FXE detected the obtained beat signal in the Λ-regime. For finding the 'zero point' of an optical cavity and measuring its frequency drift, the repetition and offset frequencies of the comb were stabilised relative to the passive hydrogen maser; a beat signal between the laser radiation and frequency comb was detected. From the dependence of the stationary frequency of this signal on cavity temperature, we determined the 'zero-point' of the latter 10.8 ± 0.2 °C. This value agrees with the result expected from properties of the materials employed and from geometry of cavity body and mirror substrates. After the cavity was stabilised at the 'zero point', the frequency drift of the

beating signal was found (340 ± 2 mHz s^{-1}), which corresponded to cavity 'shrinking'. Since the drift of a comb tooth due to a maser frequency drift is negligible as compared to this value (the maser frequency drift was directly measured while calibrating it relative to a GPS signal for two months), the latter corresponds to the drift of the cavity mode frequency. The value measured is common for 'new' cavities fabricated from ULE and is determined by material aging and relaxation of stresses.

While studying the relative instability of the laser system radiation frequency, the comb was stabilised relative to the radiation frequency of a clock laser used for spectroscopy of thulium atoms at $\lambda = 1140$ nm. This laser was arranged at a neighbouring laboratory and its radiation was delivered to the comb through a fibre, whose optical length was stabilised [35]. Beatnotes of the comb and the laser at 1140 nm were detected by the balance heterodyning method. A frequency of these beatnotes was stabilised by applying the feedback signal to the repetition rate of the comb. The comb offset frequency was locked to the pulse repetition rate. Thus, both degrees of freedom of the comb were stabilised relative to the optical reference, which provided the transfer of the relative instability of the latter to all comb teeth.

The modified Allan variance of laser system radiation beatnotes with the optically stabilised comb, normalised to the frequency of the laser system ($\lambda = 871$ nm) is presented in Fig. 3. The signal accumulation time was 10000 s. Frequency fluctuations of the compared laser systems are independent and the comb noise is low (a study of the frequency stabilities for the comb offset frequency and beatnote between the reference laser and comb showed that the comb contribution into the beatnote instability is on the order of $9 \times 10^{-18}/\tau^2$).The dependence in Fig. 3 can be interpreted as a square root from the sum of squares of modified Allan variances for the two systems. The measurement performed showed that for the time averaging interval of 0.5–50 s, the relative frequency instability of the developed laser system does not exceed 3×10^{-15} (with the linear drift excluded). In addition, a comparison of the obtained dependence of the laser system relative frequency instability with a collation result of two full-size laser systems [21] shows that metrological parameters of the laser system did not substantially worsen over the reduced mass-dimension characteristics. Note, that while taking the measurement, the optical breadboard with the laser system was rigidly mounted on the optical table with no active or passive elements for suppressing vibrations between those, the system of table active vibroisolation was deactivated, and the optical table and vacuum chamber had no isolation from acoustic vibrations. Thus, the system developed demonstrates vibration stability sufficient for operation in conventional room conditions, which is important for its employment in transportable systems.

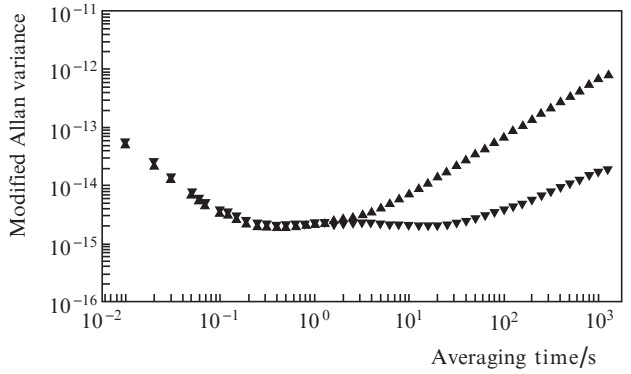

Figure 3. Relative instability of the beatnote frequency between a compact laser system at 871 nm with a mode of the femtosecond comb stabilised relative to the clock laser used for thulium atom spectroscopy at 1140 nm. Triangles with vertex up show modified Allan variance for beatnote signal; vertex down, modified Allan variance with excluded linear drift that is 340 mHz s^{-1}. The data acquisition interval is 10000 s.

The relative instability introduced by the fibre doublers, which are similar to that used in the present work and operate at the same wavelengths is less than 10^{-17} [36] at an averaging time of above 1 s; hence, one may conclude that the fundamental frequency instability level transfers to 435.5 nm without changes.

5. Conclusions

Results are presented on the development of a compact laser system with an output wavelength of 435.5 nm designed for manipulating a quantum state of an optical qubit on the $^2S_{1/2}(F = 0) \rightarrow {}^2D_{3/2}(F = 2)$ quadrupole transition in $^{171}Yb^+$ ion. The system is an improved version of those reported in [22]. The mass and volume of the system have been substantially reduced, the metrological characteristics and reliability remaining at the same level. The system demonstrated the relative instability of the output frequency of less than 3×10^{-15} at an averaging time from 0.5 to 50 s and operation without additional acoustic protection (however, in the laboratory conditions), which is important for transportable versions of such systems. The minimum of the beatnote relative instability of 2×10^{-15} is close to the thermal noise limit of the reference cavity at a wavelength of 1140 nm (1×10^{-15}) [30]. Instability of the beat signal can be affected by other factors, such as vibrations, residual amplitude modulation, and parasitic interferometers, to which the system developed is rather sensitive due to a low quality of mirrors (low transmission and finesse).

The metrological characteristics demonstrated are sufficient for controlling an optical qubit on ytterbium ion. In addition to quantum logic research, such compact systems are important in a number of scientific and practical applications, for example, precision spectroscopy of ytterbium ion aimed at verifying fundamental theories [37] and development of optical frequency standards on this ion [24, 26, 27, 38].

Acknowledgements. The work was supported by the Russian Foundation for Basic Research (Project No. 19-32-90103).

References

1. Bernien H., Schwartz S., Keesling A., Levine H., Omran A., Pichler H., Choi S., Zibrov A.S., Endres M., Greiner M., Vuletic V., Lukin M.D. *Nature*, **551**, 579 (2017).
2. Zhang J., Pagano G., Hess P.W., Kyprianidis A., Becker P., Kaplan H., Gorshkov A.V., Gong Z.-X., Monroe C. *Nature*, **551**, 601 (2017).
3. Wright K., Beck K.M., Debnath S., et al. *Nat. Commun.*, **10**, 1 (2019).
4. Landsman K.A., Wu Y., Leung P.H., Zhu D., Linke N.M., Brown K.R., Duan L., Monroe C. *Phys. Rev. A*, **100**, 1 (2019).

5. Arute F., Arya K., Babbush R., et al. *Nature*, **574**, 505 (2019).
6. Cross A.W., Bishop L.S., Sheldon S., Nation P.D., Gambetta J.M. *Phys. Rev. A*, **100**, 032328 (2019).
7. https://arxiv.org/abs/2003.01293 (2020).
8. Ziegler M., Leonhardt T. *Digit. Welt*, **3**, 50 (2019).
9. Bruzewicz C.D., Chiaverini J., McConnell R., Sage J.M. *Appl. Phys. Rev*., **6**, 021314 (2019).
10. Saffman M. *J. Phys. B: At. Mol. Opt. Phy*s., **49**, 202001 (2016).
11. Flamini F., Spagnolo N., Sciarrino F. *Rep. Prog. Phys*., **82**, 016001 (2019).
12. Wang Y., Um M., Zhang J., An S., Lyu M., Zhang J.N., Duan L.M., Yum D., Kim K. *Nat. Photonics*, **11**, 646 (2017).
13. Gaebler J.P., Tan T.R., Lin Y., Wan Y., Bowler R., Keith A.C., Glancy S., Coakley K., Knill E., Leibfried D., Wineland D.J. *Phys. Rev. Lett*., **117**, 1 (2016).
14. Harty T.P., Allcock D.T.C., Ballance C.J., Guidoni L., Janacek H.A., Linke N.M., Stacey D.N., Lucas D.M. *Phys. Rev. Lett*., **113**, 2 (2014).
15. Ratcliffe A.K., Taylor R.L., Hope J.J., Carvalho A.R.R. *Phys. Rev. Lett*., **120**, 1 (2018).
16. Lekitsch B., Weidt S., Fowler A.G., Mølmer K., Devitt S.J., Wunderlich C., Hensinger W.K. *Sci. Adv*., **3**, 1 (2017).
17. Debnath S., Linke N.M., Figgatt C., Landsman K.A., Wright K., Monroe C. *Nature*, **536**, 63 (2016).
18. Tan T.R., Gaebler J.P., Lin Y., Wan Y., Bowler R., Leibfried D., Wineland D.J. *Nature*, **528**, 380 (2015).
19. Akerman N., Glickman Y., Kotler S., Keselman A., Ozeri R. *Appl. Phys. B: Lasers Opt*., **107**, 1167 (2012).
20. Akerman N., Navon N., Kotler S., Glickman Y., Ozeri R. *New J. Phys*., **17**, 113060 (2015).
21. Berdasov O.I., Gribov A.Yu., Belotelov G.S., Pal'chikov V.G., Strelkin S.A., Khabarova K.Yu., Kolachevsky N.N., Slyusarev S.N. *Quantum Electron*., **47** (5), 400 (2017) [*Kvantovaya Elektron*., **47** (5), 400 (2017)].
22. Golovizin A., Fedorova E., Tregubov D., Sukachev D., Khabarova K., Sorokin V., Kolachevsky N. *Nat. Commun*., **10**, 1 (2019).
23. Cesare S., Allasio A., Anselmi A., Dionisio S., Mottini S., Parisch M., Massotti L., Silvestrin P. *Adv. Sp. Res*., **57**, 1047 (2016).
24. Semerikov I.A., Khabarova K.Yu., Zalivako I.V., Borisenko A.S., Kolachevsky N.N. *Bull. Lebedev Phys. Inst*., **45**, 337 (2018) [*Kr. Soobshch. Fiz. FIAN*, **45**, 14 (2018)].
25. Belotelov G.S., Sutyrin D.V., Slyusarev S.N. *Raketno-kosmicheskoe priborostroenie i informatsionnye sistemy*, **6**, 24 (2019).
26. https://www.opticlock.de/.
27. Lacroûte C., Souidi M., Bourgeois P.-Y., Millo J., Saleh K., Bigler E., Boudot R., Giordano V., Kersalé Y. *J. Phys. Conf. Ser*., **723**, 012025 (2016).
28. Cao J., Zhang P., Shang J., Cui K., Yuan J., Chao S., Wang S., Shu H., Huang X. *Appl. Phys. B: Lasers Opt*., **123**, 1 (2017).
29. Drever R.W.P., Hall J.L., Kowalski F.V., Hough J., Ford G.M., Munley A.J., Ward H. *Appl. Phys. B*, **31**, 97 (1983).
30. Alnis J., Matveev A., Kolachevsky N., Udem T., Hänsch T.W. *Phys. Rev. A: At. Mol. Opt. Phys*., **77**, 1 (2008).
31. Numata K., Kemery A., Camp J. *Phys. Rev. Lett.*, **93**, 1 (2004).
32. Legero T., Kessler T., Sterr U. *J. Opt. Soc. Am. B*, **27**, 914 (2010).
33. Rempe G., Lalezari R., Thompson R.J., Kimble H.J. *Opt. Lett*., **17**, 363 (1992).
34. Carleton H.R., Maloney W.T. *Appl. Opt*., **7**, 1241 (1968).
35. Riehle F. *Nat. Photonics*, **11**, 25 (2017).
36. Delehaye M., Millo J., Bourgeois P.Y., Groult L., Boudot R., Rubiola E., Bigler E., Kersalé Y., Lacroûte C. *IEEE Photonics Technol. Lett*., **29**, 1639 (2017).
37. Uzan J.-P. *Living Rev. Relativ*., **14** (2011).
38. Kireev A.N., Tausenev A.V., Tyurikov D.A., Shelkovnikov A.S., Shepelev D.V., Konyashchenko A.V., Gubin M.A. *Quantum Electron*., **46** (12), 1139 (2016) [*Kvantovaya Elektron*., **46** (12), 1139 (2016)].